

Final Project Report

Jeffrey Ryu

College of Engineering and Computer Science, Syracuse University

MAE 573: Application of FEA

Professor Mehmet Sarimurat

Dec. 16th, 2021

Table of Contents

Introduction	3
Mesh and Boundary Condition	5
Results	
Full	8
Fan Section	18
Modal	21
Appendix	23

Introduction

The objective of this project was to perform thermal and structural analysis of a cooling system. Ansys was used for carrying out finite element analysis. The geometry was provided as below, with a fan, casing, and a heat sink.

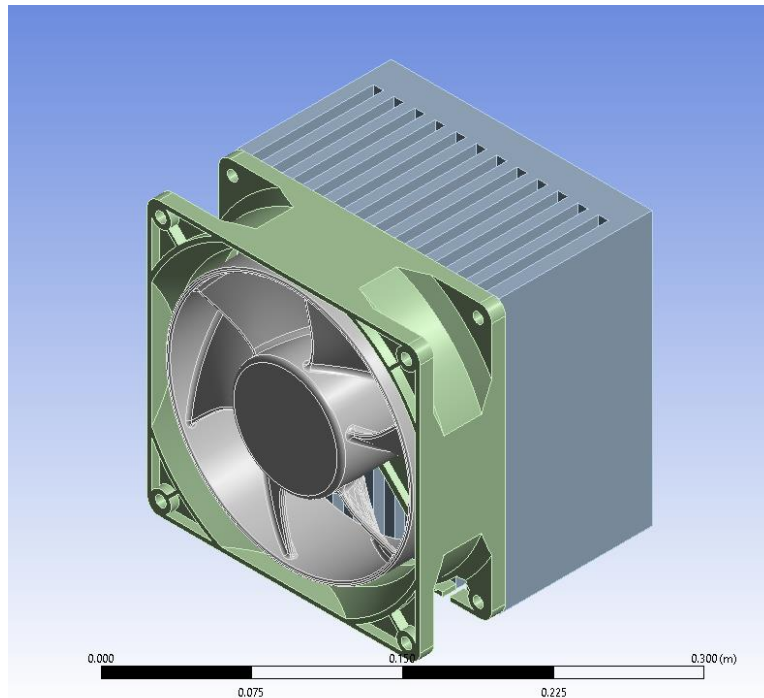


Figure 1: Geometry

The fan and its casing consisted of Glass filled Nylon with properties shown in Figure 2, and the heat sink consisted of Aluminum with properties shown in Figure 3.

Properties of Outline Row 4: Glass filled Nylon				
	A	B	C	D E
1	Property	Value	Unit	
2	<input checked="" type="checkbox"/> Material Field Variables	<input checked="" type="checkbox"/> Table		
3	<input checked="" type="checkbox"/> Density	1360	kg m ⁻³	<input checked="" type="checkbox"/>
4	<input checked="" type="checkbox"/> Isotropic Secant Coefficient of Thermal Expansion			<input checked="" type="checkbox"/>
5	<input checked="" type="checkbox"/> Coefficient of Thermal Expansion	2.56E-05	C ⁻¹	<input checked="" type="checkbox"/>
6	<input checked="" type="checkbox"/> Isotropic Elasticity			<input checked="" type="checkbox"/>
7	Derive from	Young's Modulus and Po...		
8	Young's Modulus	6.2E+09	Pa	<input checked="" type="checkbox"/>
9	Poisson's Ratio	0.35		<input checked="" type="checkbox"/>
10	Bulk Modulus	6.8889E+09	Pa	<input checked="" type="checkbox"/>
11	Shear Modulus	2.2963E+09	Pa	<input checked="" type="checkbox"/>
12	<input checked="" type="checkbox"/> Tensile Yield Strength	5.5E+07	Pa	<input checked="" type="checkbox"/>
13	<input checked="" type="checkbox"/> Compressive Yield Strength	5.5E+07	Pa	<input checked="" type="checkbox"/>
14	<input checked="" type="checkbox"/> Isotropic Thermal Conductivity	0.23	W m ⁻¹ C ⁻¹	<input checked="" type="checkbox"/>

Figure 2: Glass filled Nylon Properties

Properties of Outline Row 3: Aluminum				
	A	B	C	D E
1	Property	Value	Unit	
2	Material Field Variables	Table		
3	Density	2700	kg m ⁻³	
4	Isotropic Secant Coefficient of Thermal Expansion			
5	Coefficient of Thermal Expansion	2.36E-05	C ⁻¹	
6	Isotropic Elasticity			
7	Derive from	Young's Modulus and Po...		
8	Young's Modulus	6.98E+10	Pa	
9	Poisson's Ratio	0.33		
10	Bulk Modulus	6.8431E+10	Pa	
11	Shear Modulus	2.6241E+10	Pa	
12	S-N Curve	Tabular		
16	Tensile Yield Strength	2.76E+08	Pa	
17	Compressive Yield Strength	2.76E+08	Pa	
18	Tensile Ultimate Strength	3.1E+08	Pa	
19	Compressive Ultimate Strength	0	Pa	
20	Isotropic Thermal Conductivity	167	W m ⁻¹ C ⁻¹	
21	Specific Heat Constant Pressure, C _p	875	J kg ⁻¹ C ⁻¹	
22	Isotropic Relative Permeability	1		
23	Isotropic Resistivity	Tabular		

Figure 3: Aluminum Properties

For a modal analysis, the fan was cut radially in six pieces in cyclic pattern to make the analysis more resource efficient. *Figure 4* shows the geometry of the fan section.

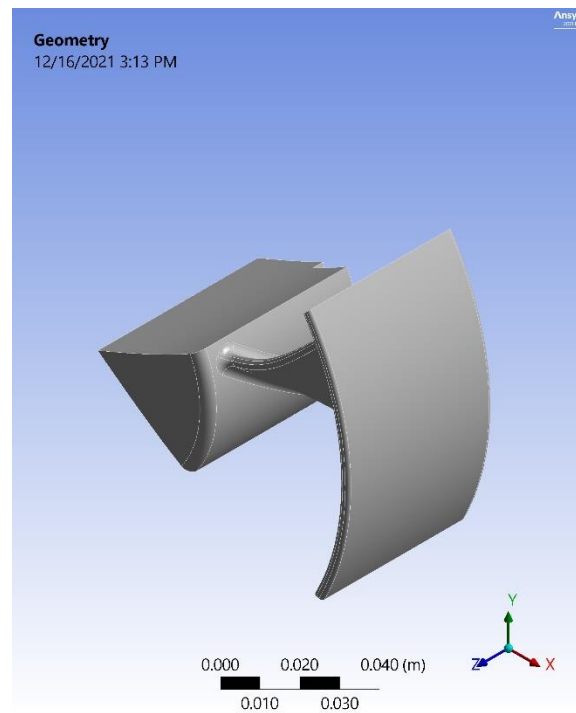


Figure 4: Fan Section

Mesh

The mesh was constructed with emphasis on the complicated geometry of the fan and its casing, while the sink with relatively simple geometry was constructed with larger and simpler mesh elements.

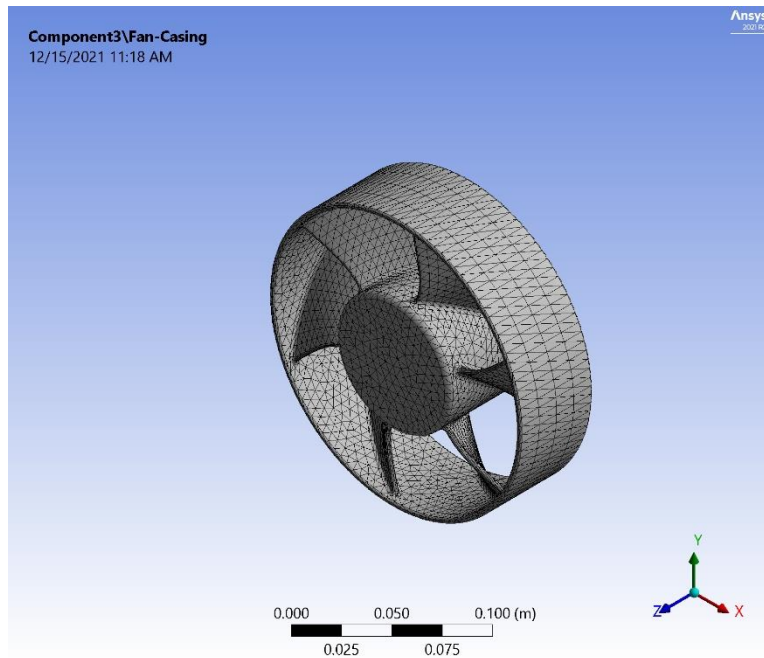


Figure 5: Initial Fan Mesh

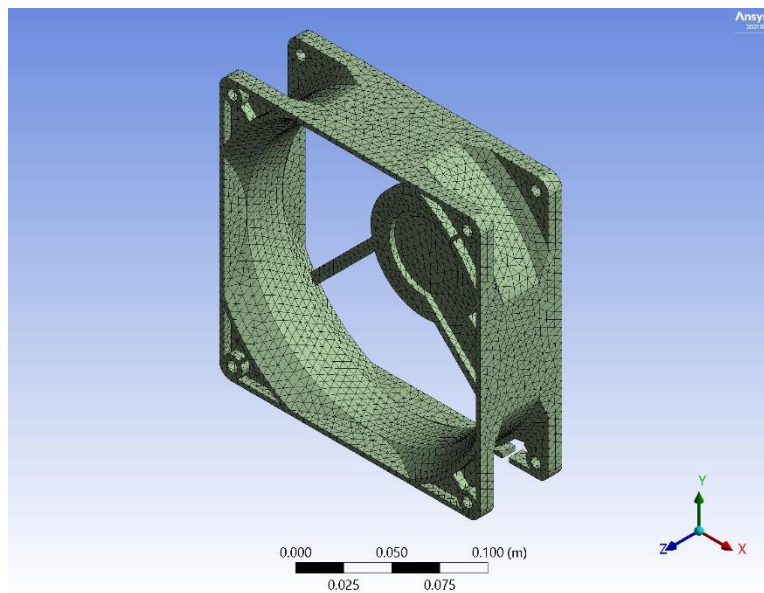


Figure 6: Fan Casing Mesh

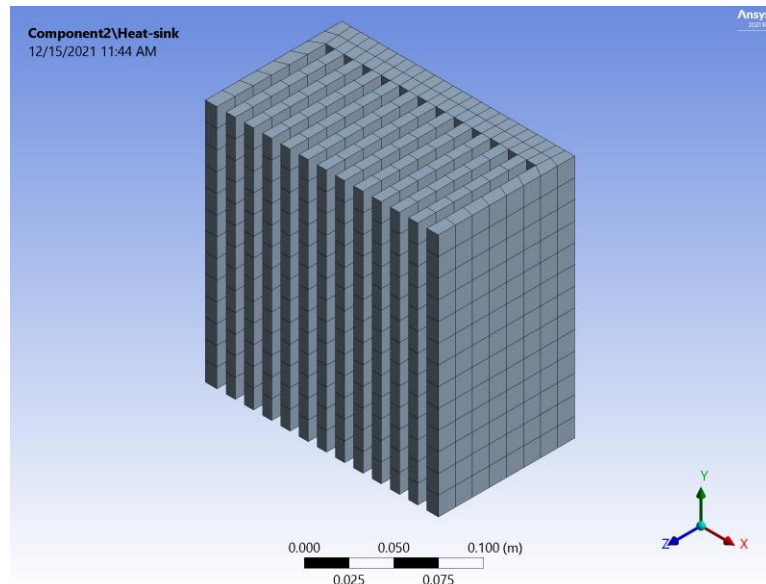


Figure 7: Sink Mesh

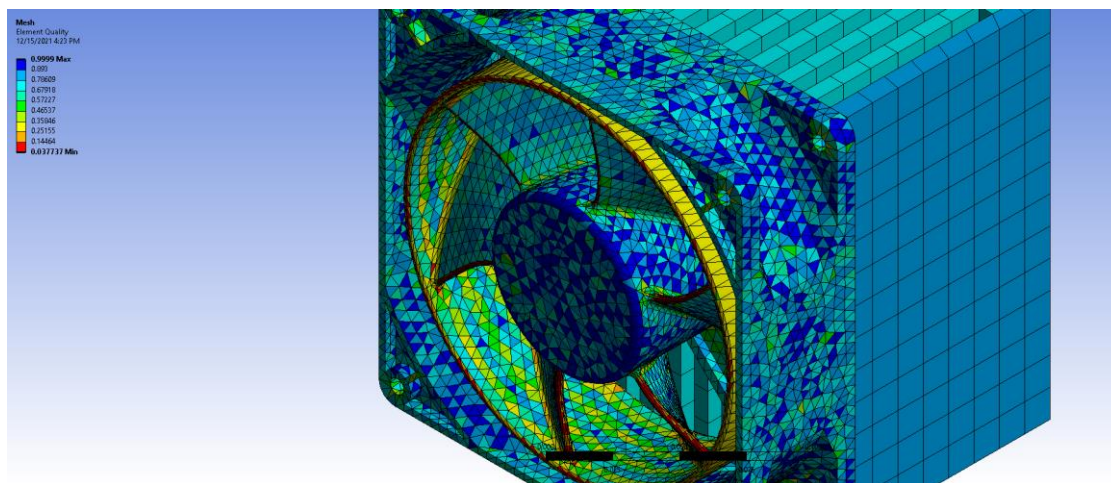


Figure 8: Mesh Quality

As shown in *Figure 8*, the mesh element quality suffers at the rounded edges of the fan blade, creating narrow elements. There are also multiple faces on the back face of the fan blades, and these can be considered as a single face using virtual topology.

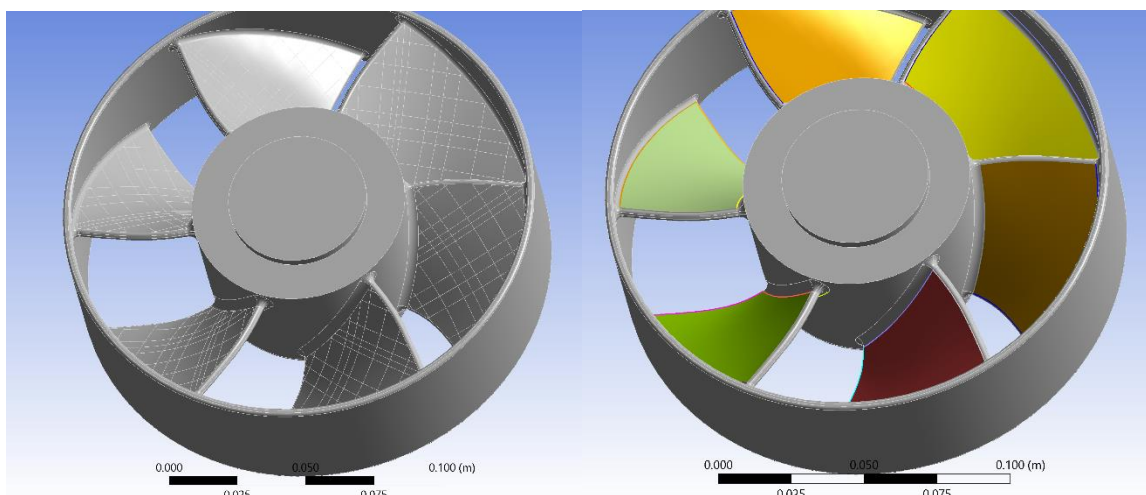


Figure 9: Virtual Topology

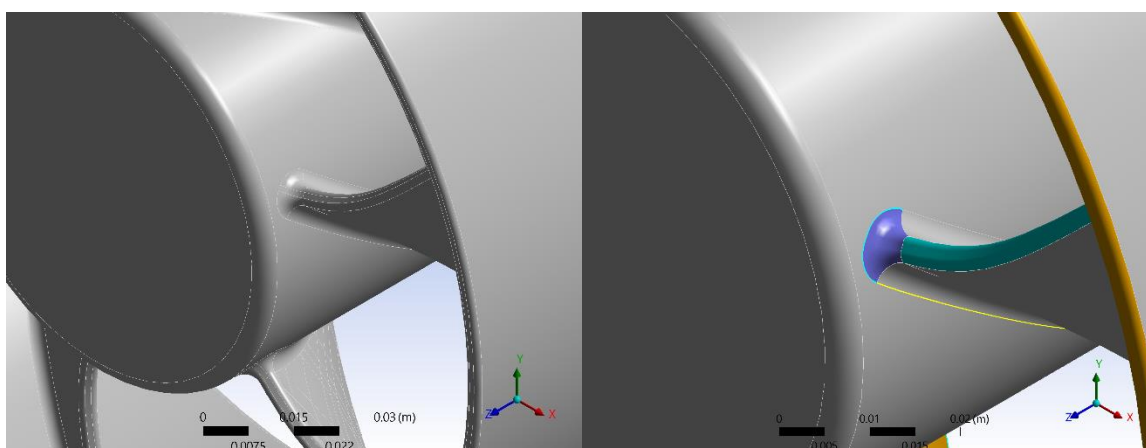


Figure 10: Virtual Topology

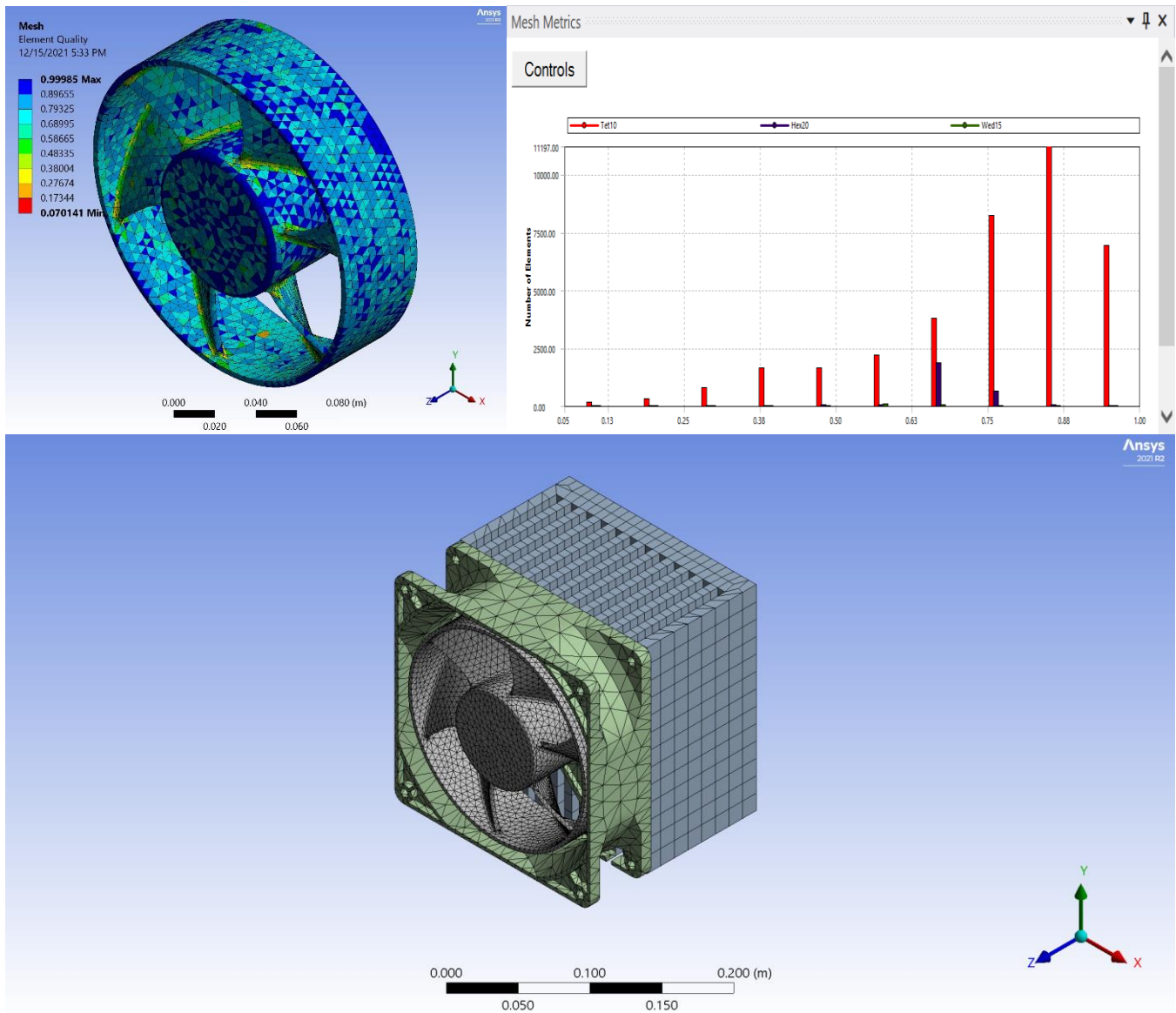


Figure 11: Final Mesh

Virtual faces were created as shown in *Figure 10* at the fillets and round edges where small faces would cause narrow and small mesh elements. This resulted in *Figure 11*, with less low-quality elements and this mesh was also used for the modal analysis. The mesh metrics also indicates that most of the mesh elements have sufficient quality. Moreover, virtual topology was used in a similar manner when generating mesh for the fan section.

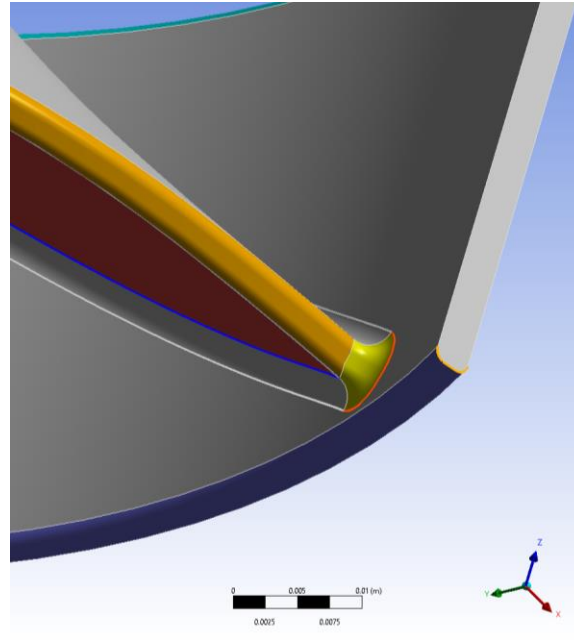


Figure 12: Fan Section Virtual Topology

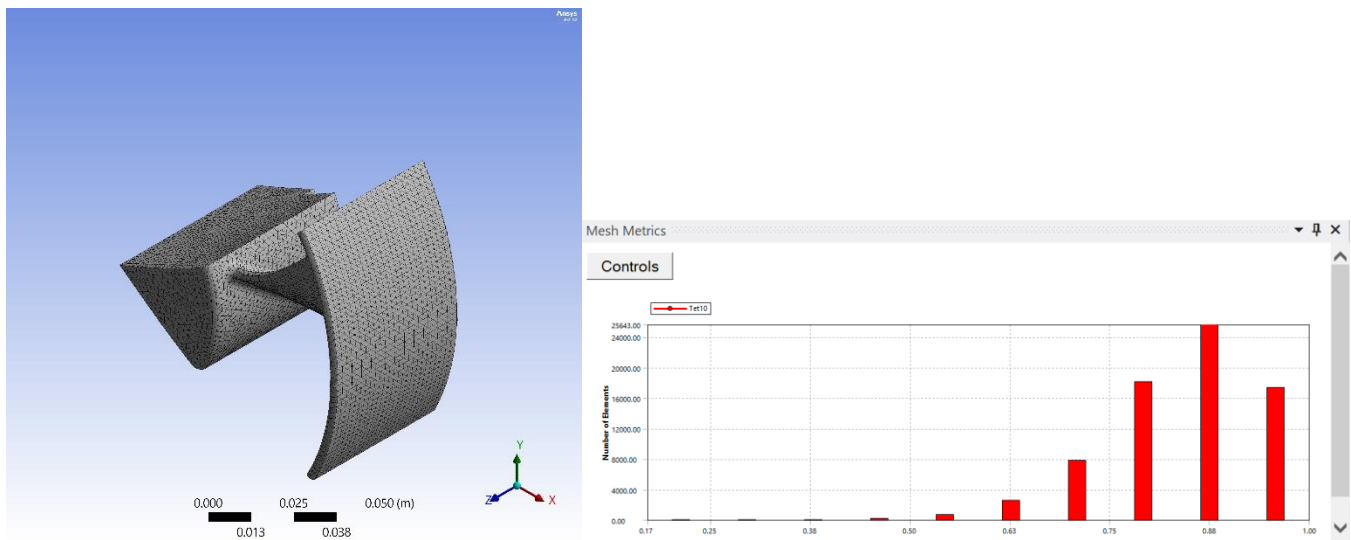


Figure 13: Mesh and Quality Metrics

The mesh for the fan section is shown as above, with the quality metrics chart suggesting that most of the elements are in the higher quality side.

On the other hand, there are several boundary conditions applied to the full cooling analysis, there exists heat flux of $\dot{q} = 2000 \text{ W/m}^2$ to the bottom of the sink, as well as convection to the fins

where the fan makes contact, of heat transfer coefficient of $h = W/(m^2 \text{ } ^\circ\text{C})$ with ambient temperature of $28 \text{ } ^\circ\text{C}$. The structural boundary conditions are defined in *Figure 14*, where the bottom of the sink is fixed with the fan rotating at 5000 RPM.

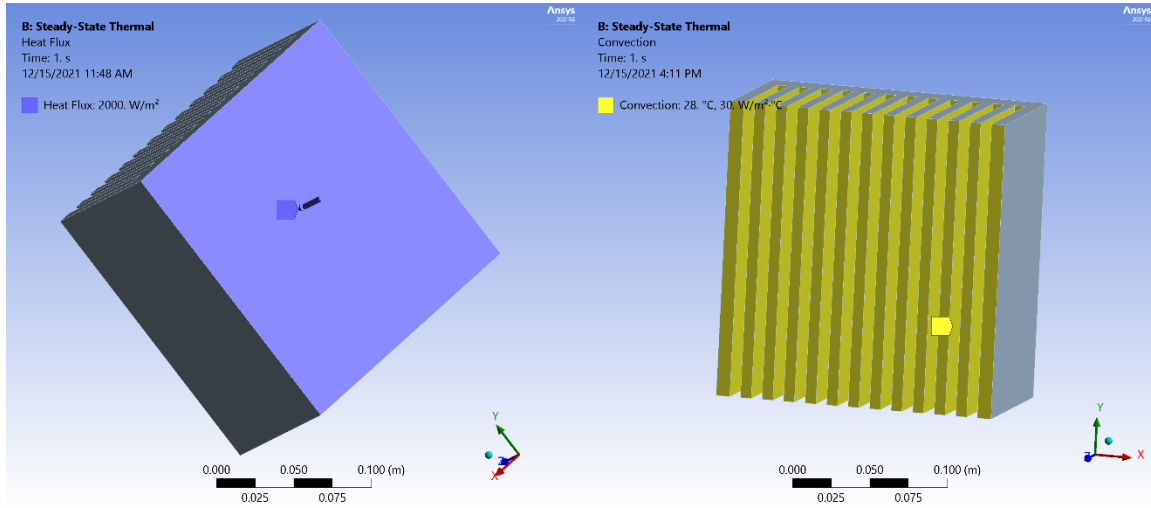


Figure 14: Thermal Boundary Conditions of Heat Sink

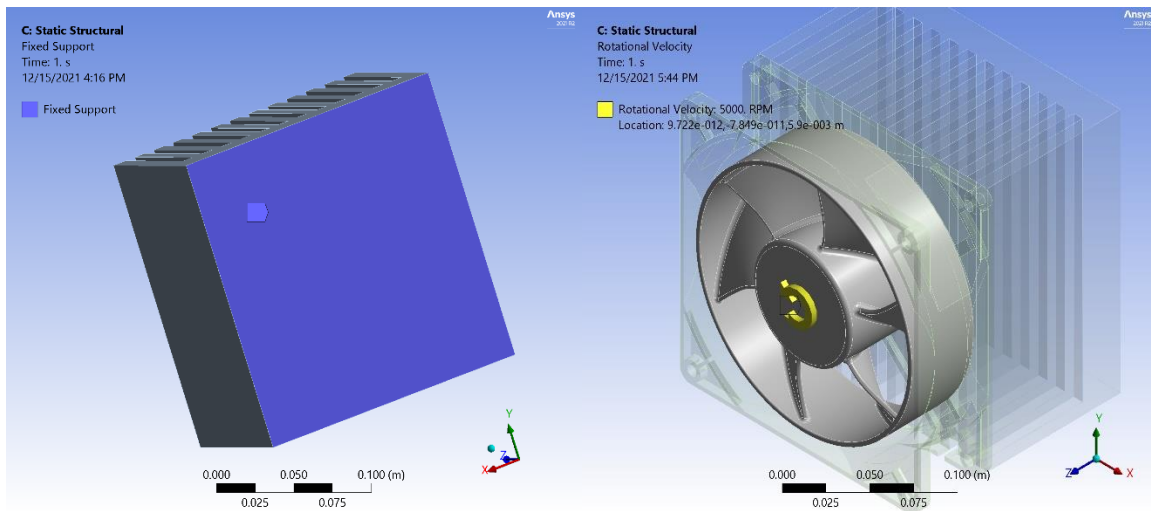


Figure 15: Structural Boundary Conditions of Heat Sink

For the fan section analysis, the cyclic pattern of the fan section is defined with the following boundaries in a cylindrical coordinate system.

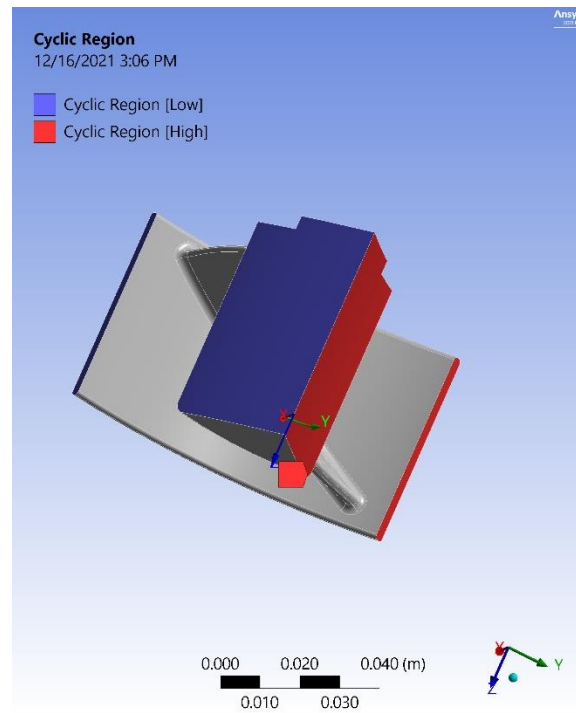


Figure 16: Fan Section Boundaries

Additionally, rotational velocity of 5000 RPM around the Z-axis was added to the fan and a fixed boundary where the fan is held by the case.

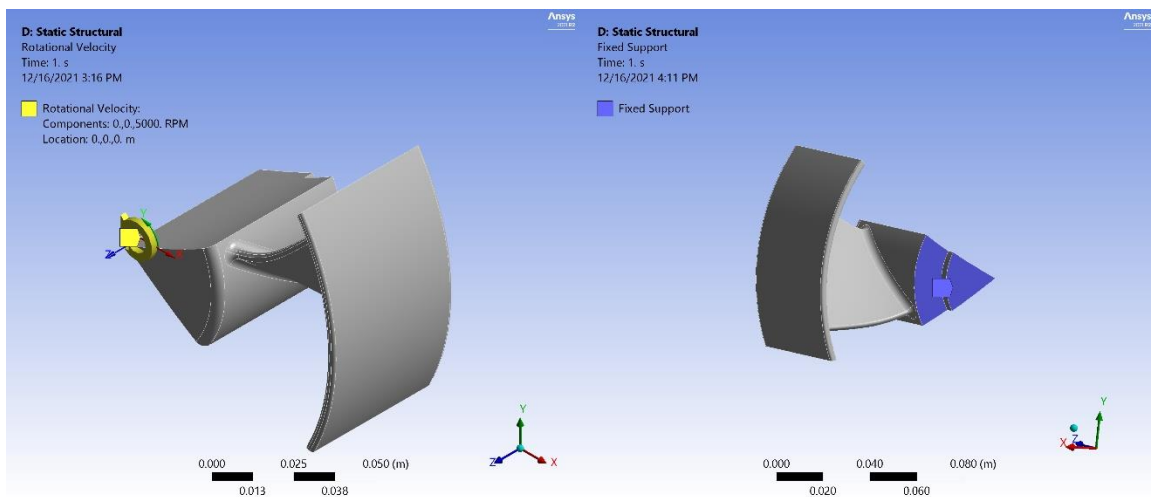


Figure 17: Fan Rotation and Fixed base

Results

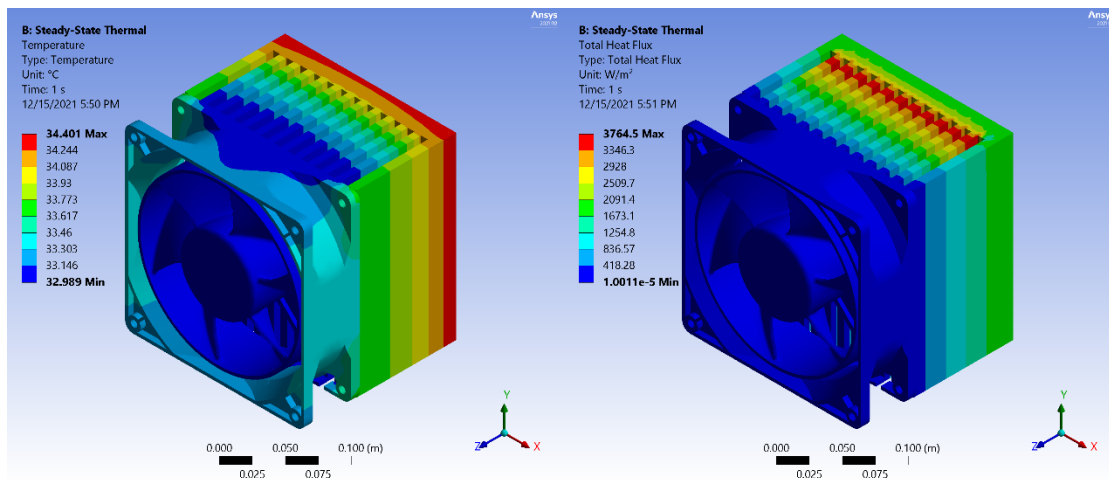


Figure 18: Thermal Results

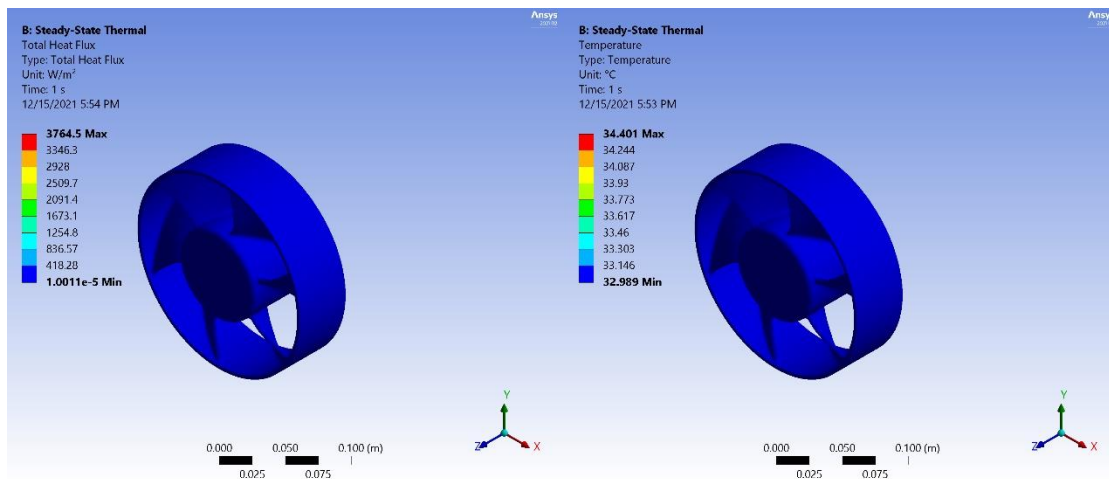


Figure 19: Fan Temperature and Flux

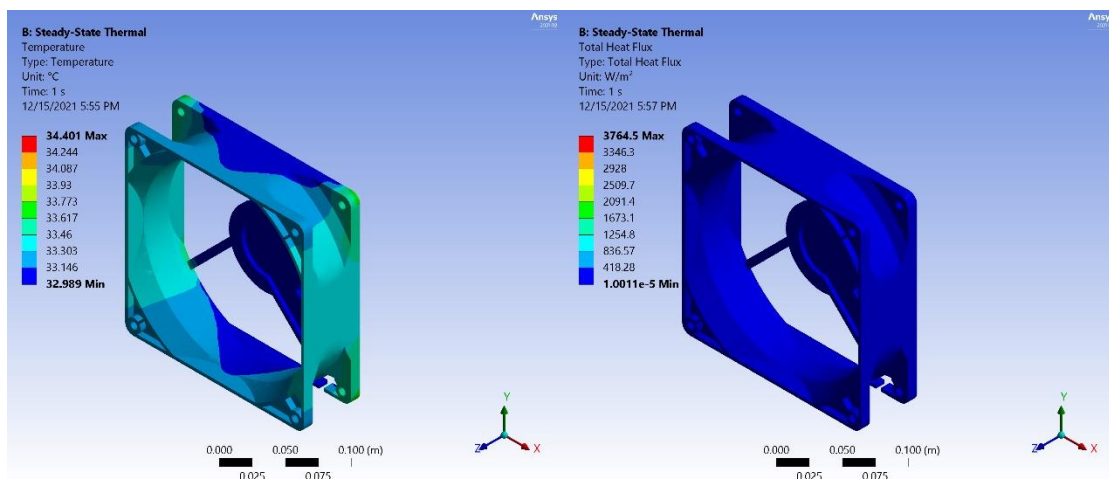


Figure 20: Case Temperature and Flux

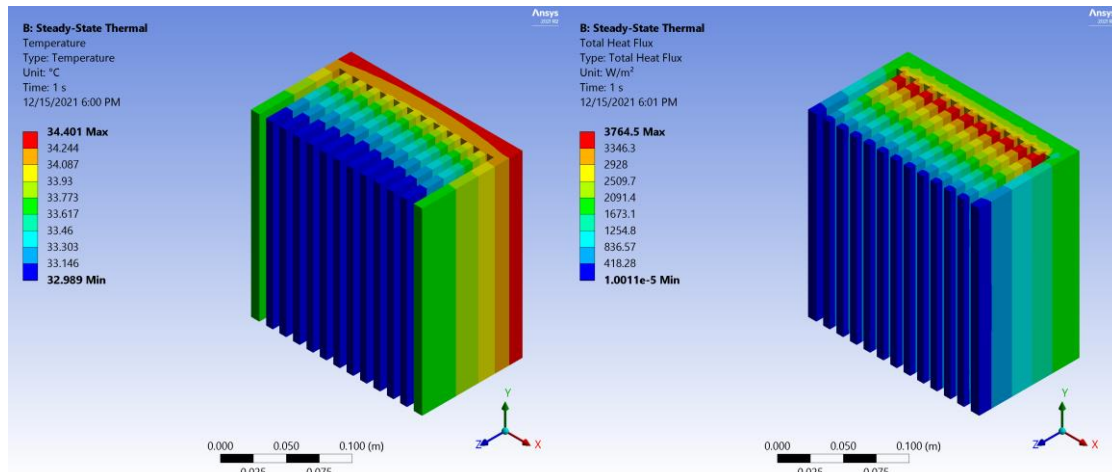


Figure 21: Heat Sink Temperature and Flux

Between the heat sink and the fan, there is a dissipation of heat transfer. Since the fan and the heat sink is not in direct contact, some of the heat transfer does not reach the fan and goes to the surrounding air through convection and radiation.

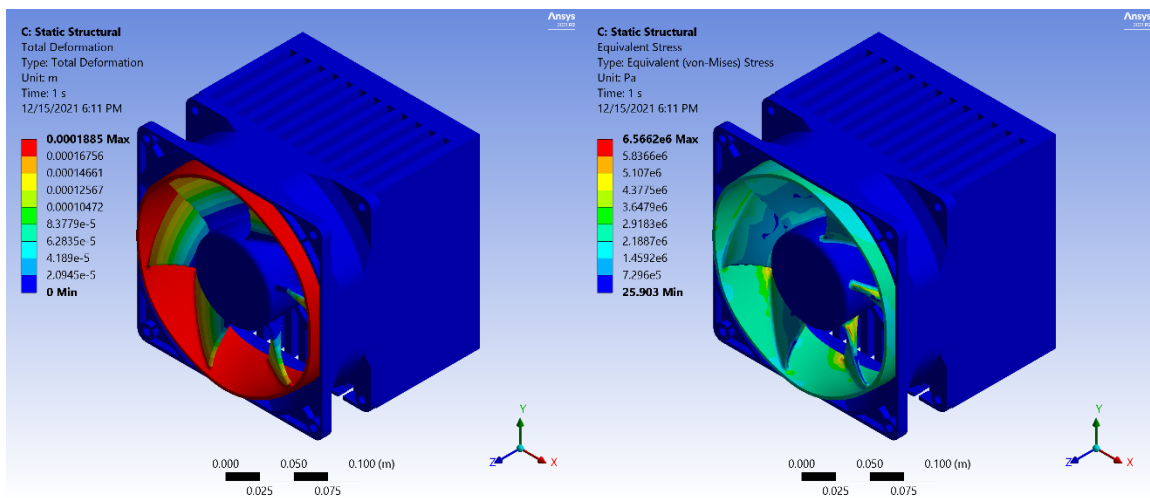


Figure 22: Total deformation and Equivalent Stress

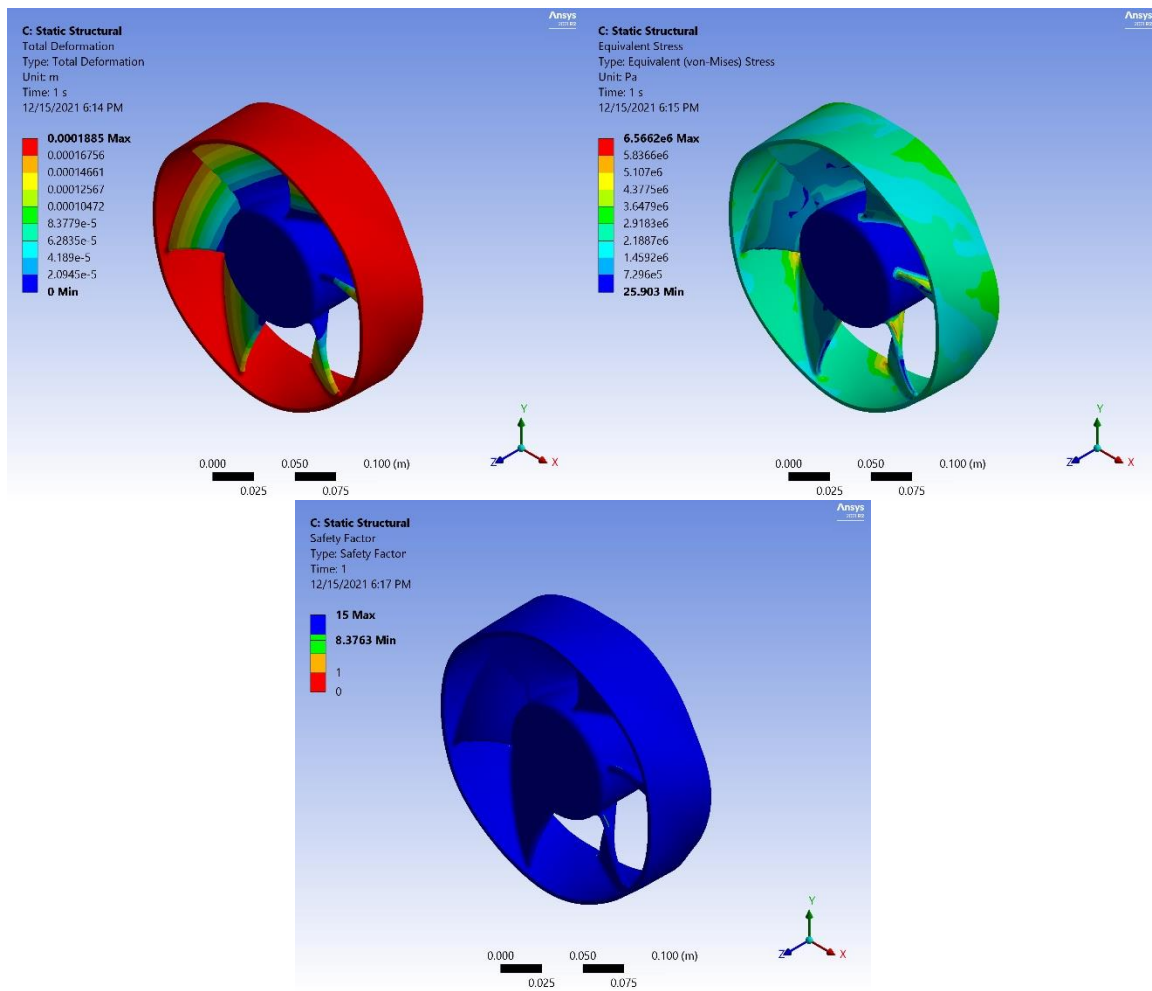


Figure 23: Total Deformation, Equivalent Stress, and Safety Factor

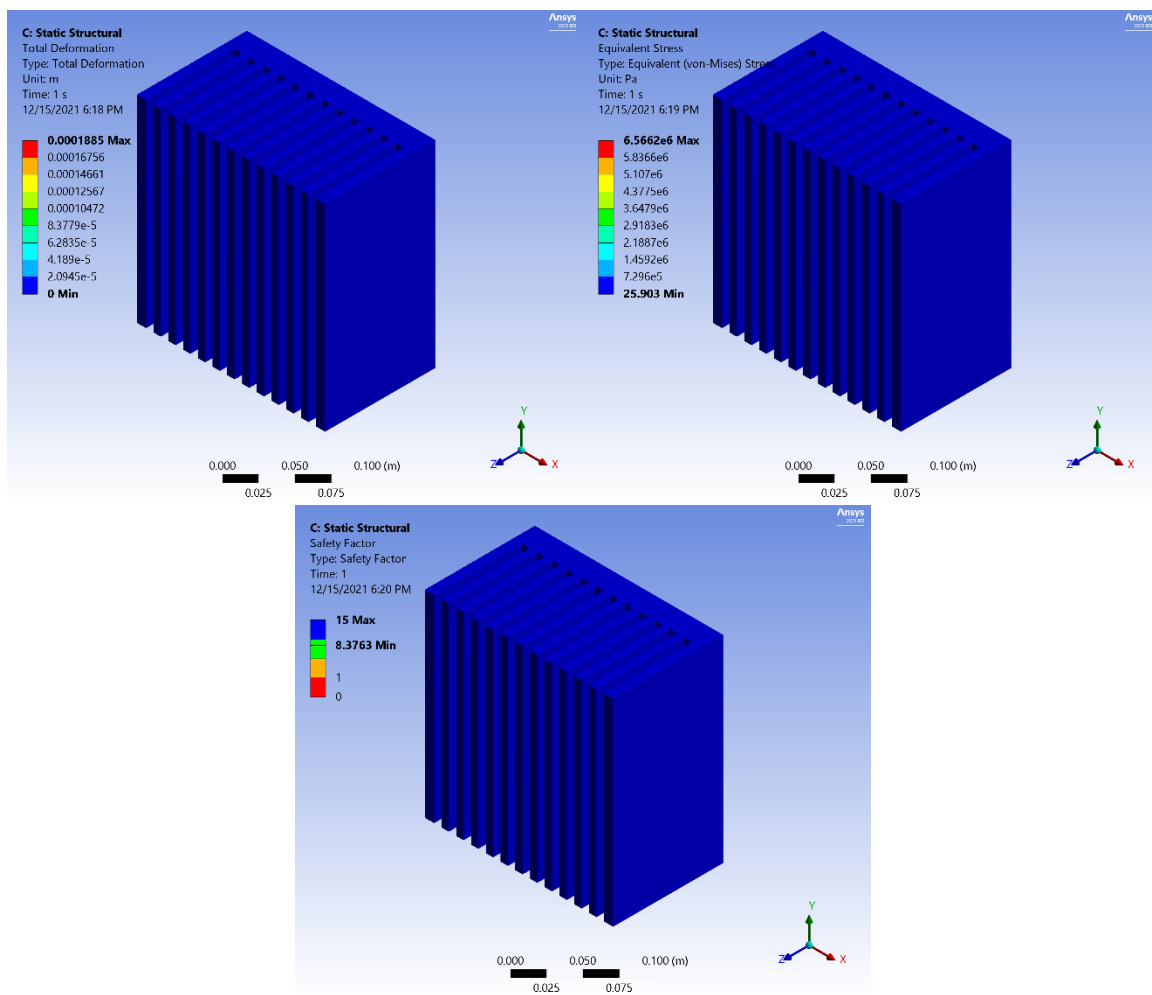


Figure 24: Total Deformation, Equivalent Stress, and Safety Factor

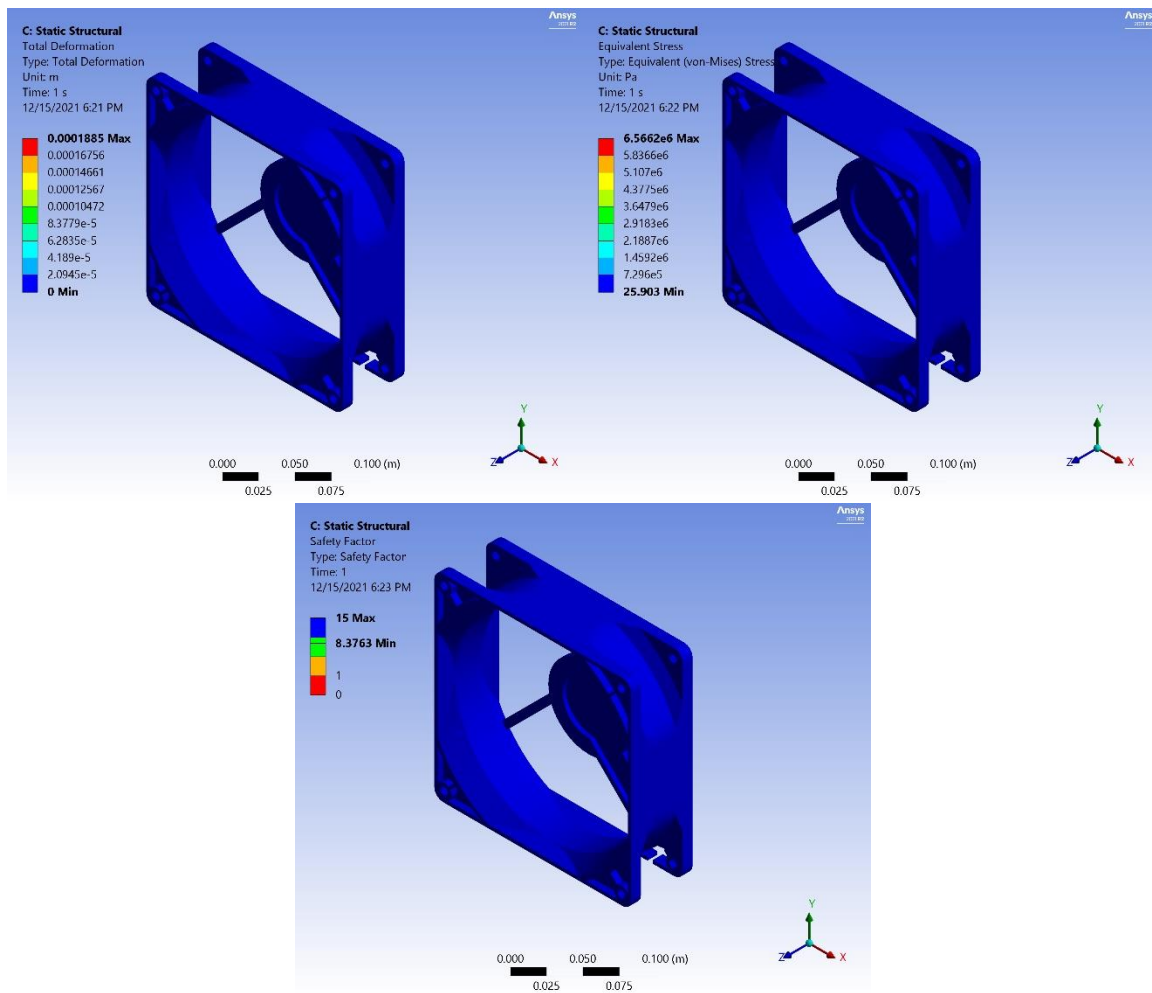


Figure 25: Total Deformation, Equivalent Stress, and Safety Factor

Based on observations of each of the cooling components, the case and heat sink experience little or no stress or deformation, while the fan experiences the most. Although there are some deformations in the fan, the stresses are not sufficiently large enough to cause any possible failures.

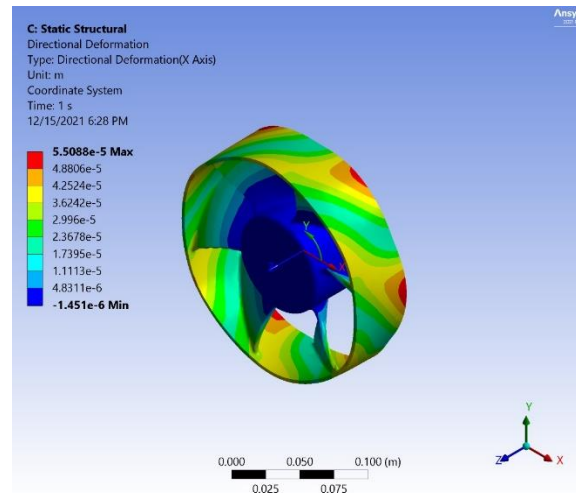


Figure 26: Directional Deformation

The maximum deformation in radial direction is measured to be 5.5088×10^{-5} meters. The initial fan's diameter is 174 mm, and the fan casing's internal diameter is 185.52 mm. The deformed fan has a maximum of 174.055088 mm diameter, which is less than the fan casing's internal diameter. The fan will not hit its case.

Fan Section

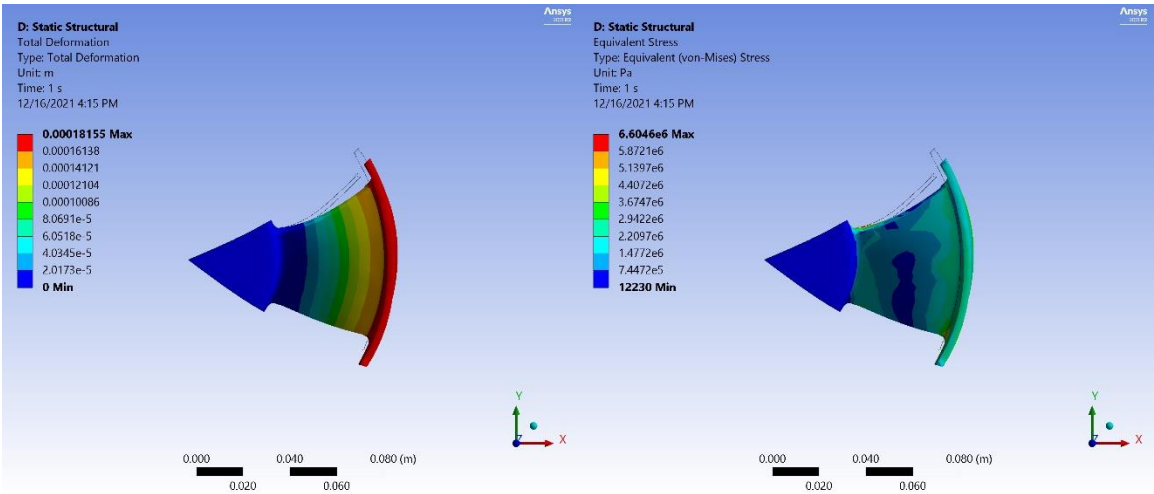


Figure 27: Fan Section’s Deformation and Stresses

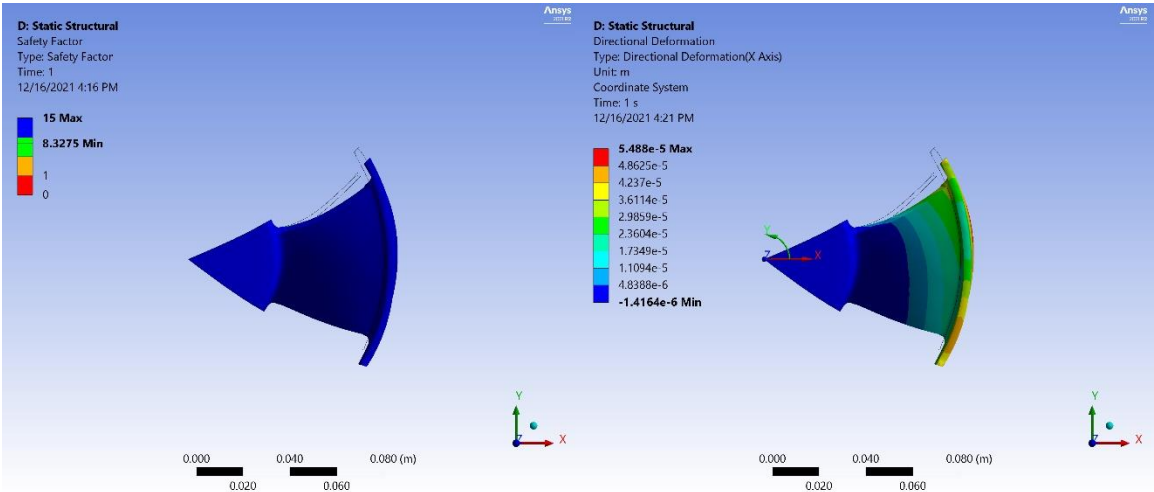


Figure 28: Fan Section’s Safety Factor and Directional Deformation

Structural analysis of the fan section shows that there is less deformation compared to the fan under heat transfer. The following *Table 1* shows the comparison of the full analysis and the fan only analysis data, and the fan under the heat transfer resulted in a slightly greater deformation.

	Fan + Heat Sink	Fan only
Max. Deformation (m)	.000185	.00018155
Max. Equivalent Stress (Pa)	6.5662e6	6.6046e6
Min. Safety Factor	8.3763	8.3275
Max. Directional Deformation (m)	5.5088e-05	5.488e-5

Table 1: Comparison of Fan

Rotational Velocity (RPM)	Maximum Deformation (m)	Average Equivalent Stress (Pa)	Minimum Safety Factor
5000	0.000182	1670431	8.327483
4000	0.000116	1069076	13.01169
3000	6.54E-05	601355.1	15
2000	2.90E-05	267268.9	15
1000	7.26E-06	66817.23	15

Table 2: Parametric Data

Consequently, the rotational velocity was parametrized, and the total deformation, equivalent stress, and safety factor was calculated as shown in *Table 2*.

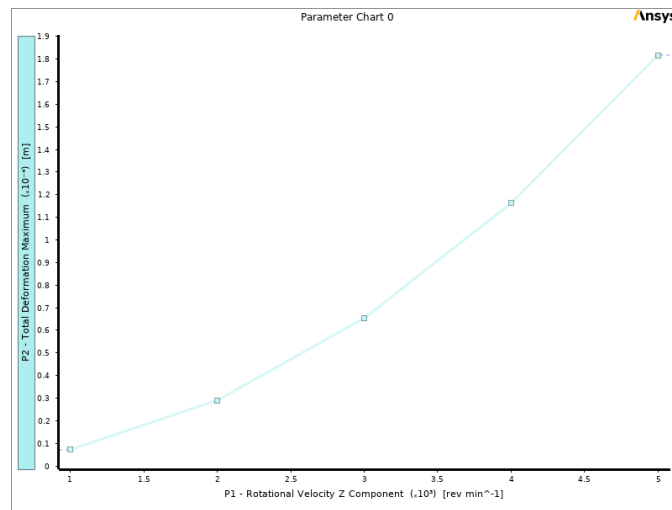


Figure 29: Rotational Velocity vs Total Deformation

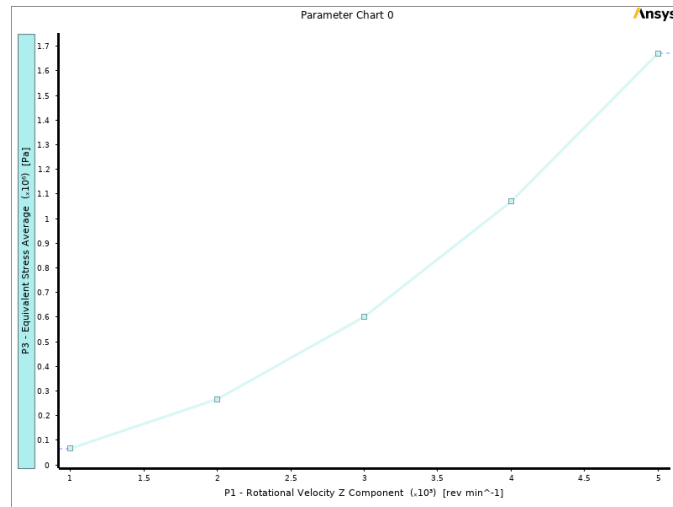


Figure 30: Rotational Velocity vs Equivalent Stress

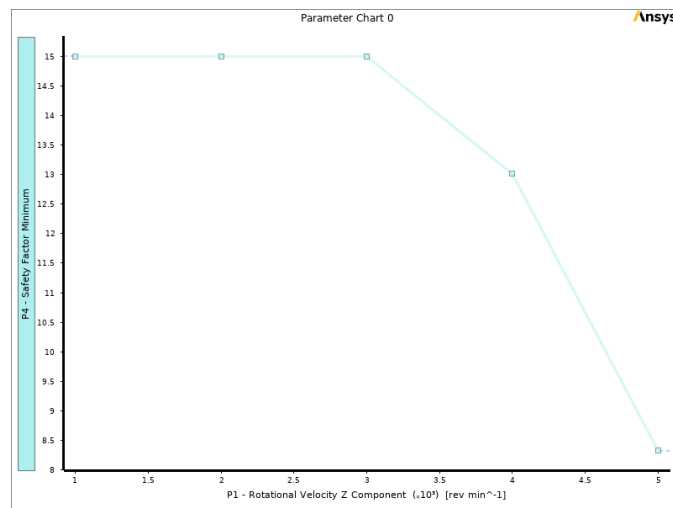


Figure 31: Rotational Velocity vs Safety Factor

The parametrized data were plotted as shown above, and the total deformation and the equivalent stress shows an exponential growth-like behavior. The maximum rotational achievable while having at least 1.5 safety factor is around 11500 RPM, and the directional deformation is 0.000290 meters. This adds about .29 mm to the fan, and the fan will not hit the casing.

Modal

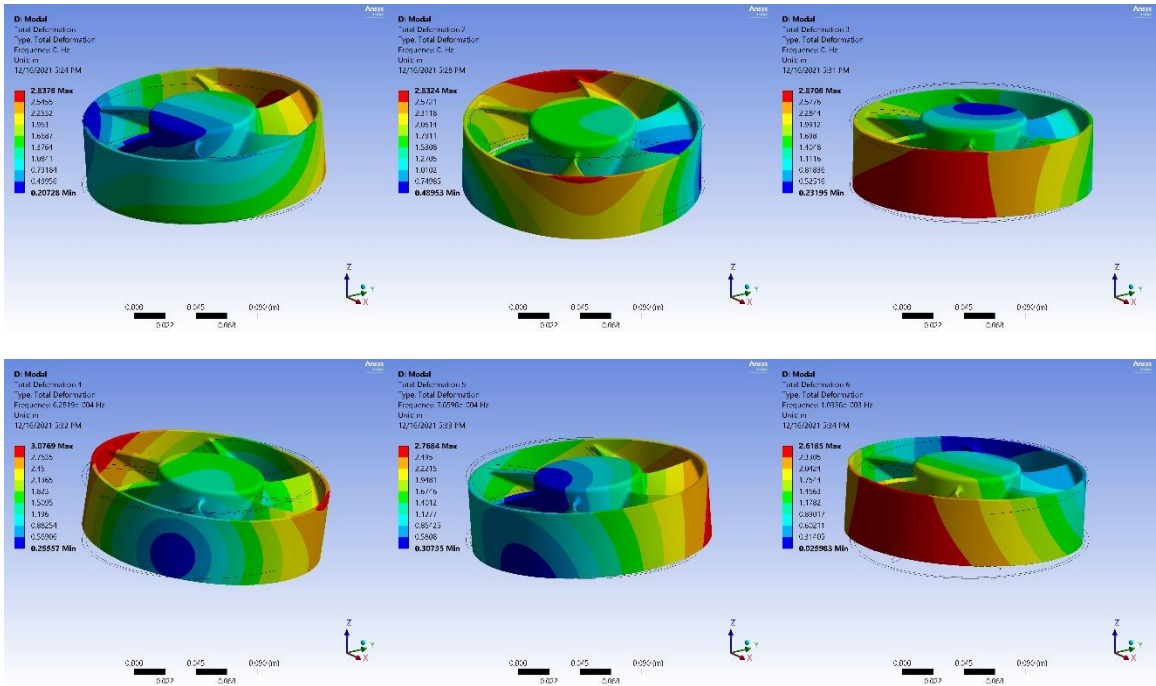


Figure 32: Mode Shapes of Fan

As shown in *Figure 32* and *33*, six mode shapes of the fan were generated. The first mode frequency occurs at 6.2819e-4 Hz.

	Mode	<input checked="" type="checkbox"/> Frequency [Hz]
1	1.	0.
2	2.	0.
3	3.	0.
4	4.	6.2819e-004
5	5.	7.6598e-004
6	6.	1.0336e-003

Figure 33: Mode Frequencies

Assuming that this frequency is insufficient and needs to be decreased by $\frac{1}{2}$, one of the ways to achieve this without changing the geometry is to increase the mass four times. The natural frequency is

determined by $\omega_n = \sqrt{\frac{k}{m}}$, thus $\frac{\omega_n}{2} = \sqrt{\frac{k}{4m}}$. Yet, another solution is to decrease the spring constant of the fan by $1/4^{\text{th}}$ by changing its material.

Appendix

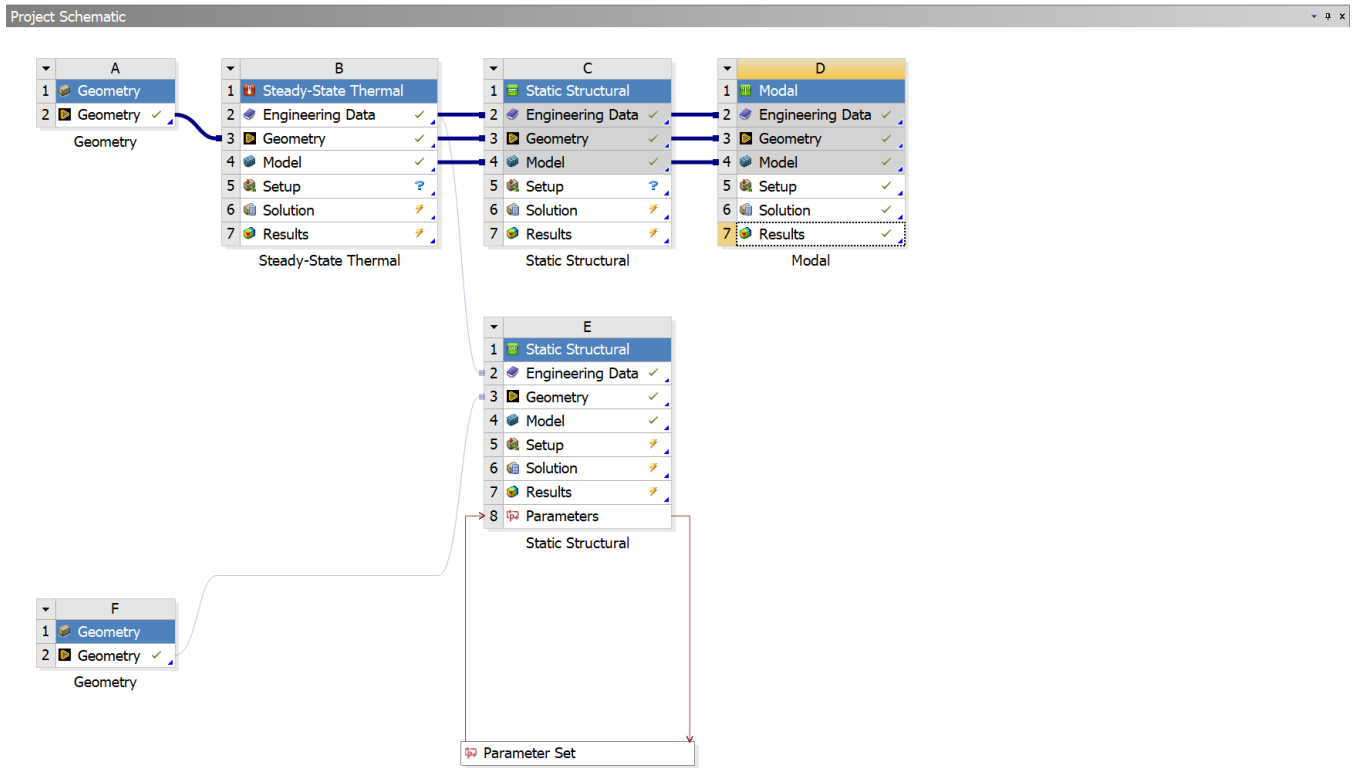


Figure 34: Workbench Schematic